ELSEVIER

Neurocomputing 50 (2003) 125–158

NEUROCOMPUTING

www.elsevier.com/locate/neucom

A computational model for the development of simple-cell receptive fields spanning the regimes before and after eye-opening

N. Rishikesh[a], Y.V. Venkatesh[a,b,*]

[a] *Computer Vision and Artificial Intelligence Laboratory, Department of Electrical Engineering, Indian Institute of Science, Bangalore - 560 012, India*

[b] *Department of Electrical and Computer Engineering, National University of Singapore, Singapore*

Received 13 April 2001; accepted 23 November 2001

Abstract

Motivated by the possible existence of post-natal cortical plasticity, we analyze Miller's (J. Neurosci. 14 (1994) 409–441) correlation-based plasticity dynamics using sinusoidal patterns of varying frequency and orientation. After demonstrating that this leads to the formation of a cluttered receptive field (RF), and analyzing the reasons therefor, we propose a Kohonen-type, response-dependent modulation of Miller's dynamics. We analyze the simulation outputs—the RF profiles and preference maps—arising from changes in the model parameters. Further, in an attempt to quantify the hypothesis that (i) spontaneous activity and (ii) visual experience play prominent roles in the (a) *establishment* and (b) *maturity of orientation selectivity*, respectively, we initialize the plasticity dynamics with developing Miller-type RFs. We interpret such an initialization to form a combined *pre-natal–post-natal* model, and quantify the relative effects of spontaneous activity and visual experience on *developing RFs* and *their preference organization*. As a next step, we analyze a possible quantification of the critical period phenomenon in the proposed model, and discuss the biological implications of such a quantification. Further, we subject the model to selective rearing by presenting it with biased visual environments. By analyzing the results, and calibrating the output using its appropriate biological counterparts, we show that the model measures up to biological realities. We also fix bounds for certain model parameters by comparing the results with biological data.

Keywords: Computational model; Correlation; Critical period; Orientation selectivity; Receptive field (RF) development; Selective rearing; Self-organization; Spontaneous neural activity; Visual experience

* Corresponding author. Tel.: +91-80-309-2572; fax: +91-80-3600444.

E-mail addresses: rishi@ee.iisc.ernet.in (N. Rishikesh), yvvele@ee.iisc.ernet.in, eleyvv@nus.edu.sg (Y.V. Venkatesh)

0925-2312/03/$ - see front matter
PII: S0925-2312(01)00701-9

1. Introduction

Miller [13] proposes a developmental origin for the Hubel–Wiesel model of oriented simple cell receptive fields (RF), and demonstrates that such RFs and their organization (into *periodic*, *continuous cortical maps*) arise naturally through an activity-dependent, correlation-based synaptic competition between ON- and OFF-center lateral geniculate nucleus (LGN) inputs to the cortex. By considering the *isotropic* intra- and inter-channel LGN activity-correlations (of *dark activity*, i.e., spontaneous neural activity in the absence of vision), he further demonstrates that oriented RFs can robustly emerge without the influence of patterned visual input. This is in agreement with the finding that orientation selectivity establishes before eye-opening [8,13,16].

However, it is also known that visual experience is crucial for the normal development of the cortex. Sharpening in orientation selectivity has been shown to be obstructed in the absence of visual experience [2,5,1]. Though major changes in preference maps are not found during the normal development of orientation selectivity [5,3,8], 'active' changes in preference maps have been reported with selective rearing [15]. This shows that the cortex, post-natally, is *still* not frozen, and is also driven by visual inputs. Further, since changes in preference maps are not substantial, it is imperative that the visual inputs *build* the developmental process on the *substrate* laid pre-natally. Moreover, selective rearing results [15] also show that the statistics of the change in preferences follow, to a certain extent, the statistics of input stimuli (in terms of orientations). This implies the *possibility* of a causal relationship between the developmental process and the statistics of the visual environment.

An important question that needs to be answered is this: *Given that an oriented receptive field can develop in the presence of isotropically correlated activity*, *how do the plasticity dynamics*, *governing such an* establishment *of orientated RFs*, *behave with non-isotropic correlations arising due to visual inputs* (*during the period after eye-opening*)?

An answer to this question is required because the responses of the neurons in the visual pathway depend upon the visual input from the environment during the stage after eye-opening, implying thereby that correlations among the neuronal responses also change. In particular, the following, more specific questions, which arise as a consequence of this change in the responses and in the correlations, provide the motivation for the present paper:

(1) What happens to the development and organization of the receptive fields?
(2) How does the correlation-based mechanism behave in such an environment? Given that visual inputs can have varied kinds of orientations and spatial frequencies, how do the developing RFs respond and change with respect to these? What kinds of changes can this bring about in the plasticity mechanisms?
(3) How do the *established*, *crude* selectivity and organization vary with the visual inputs?
(4) Given that the model quantifies a joint development of orientation selectivity in the pre- and post-natal regimes, can it quantify the critical period phenomenon?

(5) What are the biological implications of the results obtained with respect to the critical period phenomenon? What assumptions does the model make, and what is the implicit/explicit hypothesis that it follows?
(6) What changes do biases and variations in visual environment bring to the model behavior? Does the model obey the statistics of the environment? Does it measure up to the existing biological results on selective rearing [15]?
(7) Can an exact bound be set on the parameter controlling the onset of visual experience by calibrating the results against biological data?

In the course of attempting to answer these questions, we organize the paper as follows: Section 2 contains the model formulation in terms of its architecture, response equations for the lateral geniculate nucleus (LGN) and cortical neurons, and an analysis of the associated plasticity equations. Section 3 deals with the developmental process and the parametric dependence of the proposed model under normal rearing conditions. Section 4, quantifying the critical period phenomenon, presents results corresponding to dark rearing experiments on the model. Section 5 analyzes the model behavior under selective rearing, and compares the results with experimental findings in animals. Section 6 concludes the paper with discussions on issues related to the main results of the paper.

2. Model formulation

The focus of the model to be studied in this paper is the simple cells of Layer 4 of the cat's visual cortex. Though the model may be considered very general, encompassing higher mammals, we focus our attention on the cat's visual cortex for the following reasons:

(1) A majority of Layer 4 cells of the visual cortex are orientation selective in the cat, but this is not true in many other species (see [7] for details).
(2) The synaptic physiology underlying orientation selectivity is by far best studied in cats, starting from the classical experiments of Hubel and Wiesel.
(3) The results we employ for calibrating our model's outcome on selective rearing correspond to those of the cat [15].

In this section, we present the architecture of the proposed model, propose and analyze the associated plasticity equations, and study the parametric variations in them.

2.1. Model architecture

The architecture of our model is a set of ON- and OFF-center LGN neurons converging onto an array of cortical neurons. The primary visual cortex (PVC) is modelled as a 2-D array of neurons. The neurons of the PVC are innervated by the ON- and OFF-channels of the LGN, which are also modelled as 2-D arrays of neurons. The excitation from the retina to the LGN neurons is modelled as the intensity value of

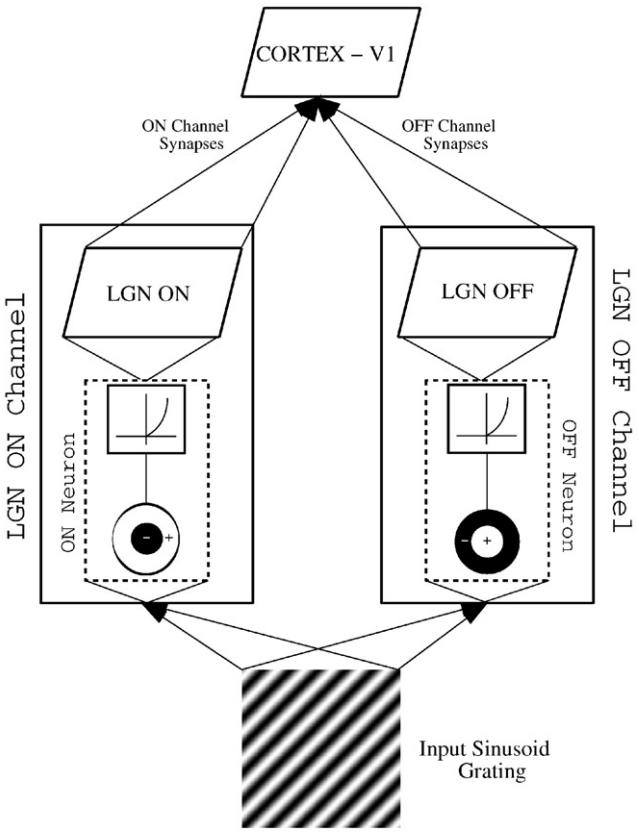

Fig. 1. The model.

the image input to the model. Fig. 1 shows a block schematic of the proposed model with the input image shown as a sinusoidal grating.

The notations and conventions used are as follows: $\mathbf{x}, \mathbf{y}$ represent cortical neurons, and α, β the LGN neurons. Retinotopy is assumed, from which follows a direct relation between positions in the LGN and the cortex, thereby allowing for the distances between the LGN and cortical neurons to be represented directly as $\mathbf{x} - \alpha$.

r_A and D_A represent the arbor radius and the arbor diameter, respectively. All LGN neurons which lie within the arbor radius r_A from cortical neuron innervate it. Essentially, r_A decides the receptive field size of the cortical neurons.

$A(\mathbf{x})$, the arbor function, describes the distance over which a single geniculate input can arborize, and make synapses with the cortex. $A(\mathbf{x} - \alpha)$ is considered to be proportional to the number of synapses connecting the ON- or OFF- input from LGN

position α to the cortical position $\mathbf{x}$. The arbor function $A(\mathbf{x})$ is set as

$$A(\mathbf{x}) = \begin{cases} 0, & |\mathbf{x}| > r_A, \\ 1, & |\mathbf{x}| < r_A(1 - c_A), \\ \dfrac{r_A - |x|}{r_A c_A} & \text{otherwise}, \end{cases} \tag{1}$$

where $c_A = 0.5$.

The difference of Gaussians (DoG) function is given by

$$\mathrm{DoG}(\mathbf{x}; r, D, \gamma) = G(\mathbf{x}; rD/2.0) - (1/\gamma^2)G(\mathbf{x}; \gamma rD/2.0) \tag{2}$$

with $G(\mathbf{x}, \sigma)$, the Gaussian, defined by

$$G(\mathbf{x}, \sigma) = \exp(-|\mathbf{x}|^2/\sigma^2). \tag{3}$$

$\mathscr{S}(\omega, \theta, \phi)$ is the sinusoid of frequency ω, orientation θ and phase shift ϕ. Explicitly, it is a sinusoidal grating, $\sin(\omega_x x + \omega_y y + \phi)$, with $\omega_x = \omega\cos(\theta)$ and $\omega_y = \omega\sin(\theta)$. Argument R refers to the random selection of that argument. For example, $\mathscr{S}(0.7, R, R)$ refers to sinusoids of all orientations (0–180°) and phase-shifts (0–2π) with spatial frequency 0.7 radians.

ω_h and ω_l represent the higher and lower bounds on spatial frequencies, and θ_h and θ_l, the higher and lower bounds on orientations of sinusoidal gratings presented to the model.

$\mathrm{Im}(i, j)$ represents the input image to the LGN channels.

$\mathscr{L}$ represents the set of co-ordinates of all LGN neurons. $\mathscr{C}$ represents the set of co-ordinates of all cortical neurons.

$*$ represents the convolution operator.

$S^{\mathrm{ON}}(\mathbf{x}, \alpha)$ and $S^{\mathrm{OFF}}(\mathbf{x}, \alpha)$ represent the synaptic strengths from position α to position $\mathbf{x}$ of the ON and OFF channels, respectively. While the lower bound value for the synapses is 0, the upper bound is set at $S_{\max} A(\mathbf{x} - \alpha)$, where $S_{\max}$ is the upper bound for synaptic values, i.e., $0 \leqslant S^{\mathrm{ON}}, S^{\mathrm{OFF}} \leqslant S_{\max} A(\mathbf{x} - \alpha)$.

Apart from the feed-forward connections from the LGN, the model also contains intra-cortical interactions. Treating them as *unmodifiable*, we model them as a "Mexican-hat" function, where the excitation of a given cortical location excites nearby cortical locations *but* inhibits distant locations [13]. Explicitly, $I(x)$, representing the intra-cortical connectivity function as a function of the distance between cortical neurons, is given by

$$I(x) = a(x)\,\mathrm{DoG}(x; r_I, D_I, \gamma_I) \tag{4}$$

with $D_I = 13$, $\gamma_I = 3$ and $r_I = 0.3$ (see [13]). The function $a(x)$ is used to reduce the amount of inter-cell interactions relative to intra-cell interactions, and $a(0) = 1$; $a(x) = a_\mathrm{l} < 1$ for $x > 0$, $a_\mathrm{l} = 0.5$.

2.1.1. The LGN

The LGN ON- and OFF-channels are modelled as a 2-D array of neurons. These neurons operate on the input image, and are modelled using the DoG functions. Explicitly, the model functions for the ON- and OFF-channel LGN neurons are given by

$$H_{\mathrm{l}}^{\mathrm{ON/OFF}}(\mathbf{x}) = +/- \mathrm{DoG}(\mathbf{x}; r_{\mathrm{l}}, D_{\mathrm{l}}, \gamma_{\mathrm{l}}), \tag{5}$$

where D_{l} is the receptive field size of the LGN neurons. In the simulations presented, $D_{\mathrm{l}} = 7$, $\gamma_{\mathrm{l}} = 1.3$ and $r_{\mathrm{l}} = 0.269$. In our experiments, we have considered the size of the cortical receptive field as 13. Considering that the LGN RF size has to be relatively smaller than this, we set D_{l} at 7. The values for γ_{l} and r_{l} are chosen in order to set the sum of the mask to zero, so that neurons having their receptive fields over uniform regions of the input image produce no excitation.

As the extracellular response measurements (i.e., firing rates) are, by definition, positive, we have to account for the negative responses arising from such a model. To this end, we employ a *half-squaring* model similar to the one studied by Heeger [10] who hypothesizes simple cells in the striate cortex as rectified linear operators to address negative responses of neurons. Explicitly, he employs half-wave rectification, followed by squaring, and shows that a cell's firing rate depends on the squared output of the underlying linear stage. Reviewing the physiological measurements, he concludes that the hypothesis is supported by the data. *In our experiments*, we employ a similar model for the LGN neurons, and feed the DoG outputs to a half-squarer. We use its outputs as inputs to the cortical neurons. See Fig. 1 which shows the ON- and OFF-LGN neurons modelled with DoG followed by a half-squarer. The output of a ON/OFF-LGN neuron is then given by

$$O_{\mathrm{l}}^{\mathrm{ON/OFF}} = \mathscr{H}(\mathrm{Im} * H_{\mathrm{l}}^{\mathrm{ON/OFF}}) \tag{6}$$

where $\mathscr{H}$ represents the half-squarer, given as

$$\mathscr{H}(x) = \begin{cases} x^2 & x > 0, \\ 0 & \text{otherwise.} \end{cases} \tag{7}$$

2.1.2. The PVC

The responses of the ON- and OFF-channels of the LGN to the input image, then, excite the simple cells of the PVC. The response of a cortical neuron to its input stimuli is modelled as a sum of two terms. The first term corresponds to the excitation from the LGN, while the second is due to the intra-cortical interaction.

The excitation from the LGN layers is modelled as

$$E_{\mathrm{l}}(\mathbf{x}) = \sum_{\alpha \in \mathscr{N}} O_{\mathrm{l}}^{\mathrm{ON}}(\alpha) S_n^{\mathrm{ON}}(\mathbf{x}, \alpha) + O_{\mathrm{l}}^{\mathrm{OFF}}(\alpha) S_n^{\mathrm{OFF}}(\mathbf{x}, \alpha), \tag{8}$$

where

$$S_n^t(\mathbf{x}, \alpha) = \sqrt{\frac{(S^t(\mathbf{x}, \alpha))^2}{\sum_{\alpha \in \mathscr{N}} (S^t(\mathbf{x}, \alpha))^2}},$$

$t \in \{\mathrm{ON}, \mathrm{OFF}\}$ and $\mathscr{N} = \{\beta\colon |\beta - \mathbf{x}| \leqslant r_A\}$.

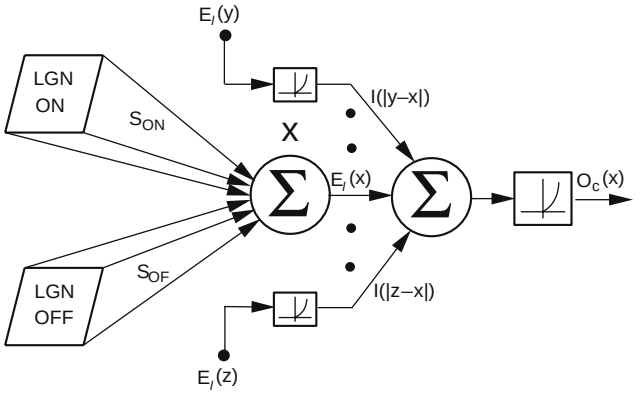

Fig. 2. Model of a cortical neuron.

The excitation/inhibition from the other cortical cells is given by

$$E_c(\mathbf{x}) = \sum_{\mathbf{y}\neq\mathbf{x}} I(|\mathbf{y}-\mathbf{x}|)\mathscr{H}(E_l(\mathbf{y})). \tag{9}$$

The sum of the above two terms, (8) and (9), yields the underlying linear sum for a given cortical neuron. In order to calculate the firing rate, we employ a strategy similar to the one employed for LGN neurons, and pass the linear sum through a half-squarer. The response of a cortical neuron at position $\mathbf{x}$ is then given by

$$\begin{aligned} O_c(\mathbf{x}) &= \mathscr{H}(E_l(\mathbf{x}) + E_c(\mathbf{x})) \\ &= \mathscr{H}\left(E_l(\mathbf{x}) + \sum_{\mathbf{y}\neq\mathbf{x}} I(|\mathbf{y}-\mathbf{x}|)\mathscr{H}(E_l(\mathbf{y}))\right). \end{aligned} \tag{10}$$

See Fig. 2 for a graphical illustration of this equation.

2.2. DoG vs. sinusoidal correlations

It is generally acknowledged that visual experience is not an essential component for the *establishment* of orientation selectivity or of its columnar organization (see [4,14,8,16]). Based on this and on the hypotheses that *endogenous, spontaneous neural activity within the visual pathway drives the establishment of orientation selectivity and columns* (see [14,17]), Miller [13] proposes a computational model for the development of oriented receptive fields and organized columns in the presence of unoriented, isotropically correlated patterns of spontaneous neural activity.

Miller [13] also proposes a developmental origin for the Hubel–Wiesel model, and presents evidences on the convergence of ON and OFF LGN cells to the orientation selective layers in the PVC. He shows that orientation-selective receptive fields and their organization into continuous periodic arrangements of preferred orientations across the

cortex arise naturally through an activity-dependent, correlation-based synaptic competition between ON- and OFF-center inputs to the PVC.

The correlations among the spontaneous neural activities of the ON- and OFF-center neurons of the LGN guide the developmental process. The intra-channel input correlations, C^{tt}, $t \in \{\mathrm{ON}, \mathrm{OFF}\}$, of the LGN are assumed to be equal (for both ON- and OFF- channels), and modelled as DoG functions. (Evidences for this and other assumptions of the model are analyzed in [13].) Further, the inter-channel input correlations, $C^{t_1 t_2}$, $t_1, t_2 \in \{\mathrm{ON}, \mathrm{OFF}\}$ where $t_1 \neq t_2$, are also assumed to be equal, and are modelled to be the negative of one-half of the intra-channel correlation function. Explicitly, the intra-channel correlation function is given by:

$$C^{tt}(\mathbf{x}) = \mathrm{DoG}(\mathbf{x}; r_C, D_A, \gamma_C) \tag{11}$$

and the inter-channel correlation function by

$$C^{t_1 t_2}(\mathbf{x}) = -0.5 C^{tt}(\mathbf{x}). \tag{12}$$

The plasticity equation analyzed by Miller is

$$\Delta S^{\mathrm{ON}}(\mathbf{x}, \alpha)|_U = \eta A(\mathbf{x} - \alpha) \sum_{\mathbf{y}, \beta} I(|\mathbf{x} - \mathbf{y}|)[C^{\mathrm{ON,ON}}(\alpha - \beta) S^{\mathrm{ON}}(\mathbf{y}, \beta) \times C^{\mathrm{ON,OFF}}(\alpha - \beta) S^{\mathrm{OF}}(\mathbf{y}, \beta)]. \tag{13}$$

After demonstrating that oriented receptive fields can develop with such a plasticity dynamics and DoG correlations, Miller [13] declares that the difference correlation function, *but not* the individual correlation functions, is the key determinant of the developmental process. The difference correlation function $C^{\mathrm{D}}(\mathbf{x}) = C^{tt}(\mathbf{x}) - C^{t_1 t_2}(\mathbf{x})$ gives the degree to which two inputs of the same center-type with a given retinotopic separation are better correlated with one another than with an input of the opposite center-type at the same separation. Oriented receptive fields are formed if (i) C^{D} changes sign with distance, so that, at small distances, similar inputs are better correlated, but, at larger distances, inputs of opposite-type are better correlated, and (ii) the sign change takes place within the arbor radius. These constraints are taken care of by the above definition of the correlation functions and an appropriate selection of parameters [13].

2.2.1. Miller's rule with sinusoidal correlations

Though the establishment of orientation selectivity may not require visual experience, it is well-known that oriented receptive fields undergo, *post-natally*, substantial modifications—*sharpening of selectivity* [2,5,1,8] and *re-organization of preference maps* (with biased rearing [15]). It is also known that visual experience is mandatory for the normal development of the visual cortex [2,1,16]. This indicates that the PVC is not *frozen* at birth, and its development *is also* driven by visual inputs. After eye-opening, the responses of the neurons in the visual pathway depend upon visual input from the environment. A consequence is that the correlations among the responses of the LGN channels will also depend on visual inputs. In order to assess the effect of such a change on the developmental process, we analyze, in this section, the

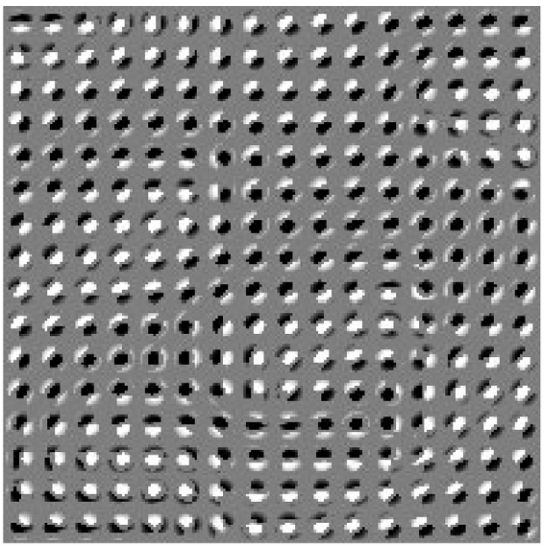

Fig. 3. Typical RF profiles obtained with sinusoidal correlation and Miller-type plasticity.

effect of correlation functions with different asymmetries—*sinusoidal gratings of varied frequencies*, *orientation and phase shifts*—on (13).

As a first step towards the analysis of the correlation framework in the phase after eye-opening, we execute Miller's algorithm with sinusoidal correlations, *but* with all the other parameters and the update equation remaining the same. By feeding the system with sinusoidal gratings of different (a) *frequencies*, (b) *orientations*, and (c) *phase shifts*, we update the synaptic weights as in (13). Explicitly, the DoG correlations, which are employed in Miller's scheme, are replaced by the instantaneous correlations of the sinusoidal gratings presented (i.e., the cosinusoid of corresponding frequency and orientation).

The results obtained with sinusoids $\mathscr{S}(0.4, R, R)$–$\mathscr{S}(0.8, R, R)$ indicate that such a change in correlations does not improve the selectivity behavior of the cells [1] but, *on the contrary*, reduces it. After computing the degree of orientation selectivity in the manner of [13], it is found that the mean degree of orientation selectivity (MDOS) corresponding to the map obtained with DoG correlations is 0.1809 (min: 0.0005, max: 0.326) while that corresponding to sinusoidal correlations is 0.119628 (min: 0.00116, max: 0.3127). It should be noted here that the learning rate parameter η was set to a very low value (0.0001) so that the network can 'see' a number of sinusoids before convergence.

Typical receptive field patterns obtained with such a simulation are shown in Fig. 3. It may be observed from the figure that the receptive fields are *cluttered*. A plausible

[1] In both cats and ferrets, sharpening of selectivity has been reported during the normal developmental period with visual experience. This does not occur with binocular deprivation, leading to the hypothesis that sharpening is based on visual experience [5].

reason for such a clutter and for the inability of Miller's plasticity rule to improve MDOS with varying sinusoidal inputs is as follows:

The input sinusoids vary in frequency, phase and orientation. But, the update rule has no mechanism to identify the neuron(s) which respond maximally to a given grating. Because of this and the relatively global update mechanism employed, each of the sinusoids modifies the RF profiles, corresponding to its frequency, phase and orientation, irrespective of the cell's existing preferences. This, in turn, '*confuses*' the cell's preferences each time it is updated, thereby leading to the clutter.

Hence, it is essential that the update mechanism takes into account the existing preferences of the cell. This requires the update scheme to be dependent on the *responses* of the various cells to a given input. (The existing preferences may be due to previous iterations of the algorithm or due to an initialization of the RFs (see Section 3).) However, the question on the biological feasibility of such a requirement arises. It may be argued that such a response-driven update is essential and feasible because:

(a) There exists a competition among different orientations for cortical area. This may be observed from selective-rearing experiments, where the reared orientation occupies twice as much cortical area as its orthogonal counterpart [15].
(b) Organization of preferences (i.e., the preference map) does not undergo major changes in the post-eye-opening period with normal visual experience [5,3]. This means that the post-eye-opening period updates are also driven by the existing cell preferences.
(c) The competition for trophic factors, which play crucial roles in neural development and are the determinants of critical periods, is dependent on activity [1]. This suggests the interpretation that the changes in synaptic efficacy would be concentrated in the neighborhood of the cell with the maximal response to a given input [11].

2.2.2. Kohonen-type modification

An important result of the last section is that a multi-sinusoidal environment requires a response-regulated plasticity rule for normal RF development. We now propose a Kohonen-type bubble mechanism as the "modulation" to a correlation-based update-rule similar to (13), which may be interpreted as a *unification* of correlation-based plasticity rules and self-organizing dynamics. Such an experience-dependent self-organizing scheme encompasses *two kinds of competitions*:

(1) Competition among the ON- and OFF-LGN channels to define the ON–OFF-subregions in the cortical neuron; and
(2) Competition among the cortical neurons to represent a particular orientation.

The former is an activity-dependent competition among the LGN ON- and OFF-center inputs as in Miller's case. This is enforced by subtractive normalization of synapses so that a synapse gains only from the other's loss. The latter is based on the responses of the cortical neurons (as in (10)) to an input visual pattern. The neuron which elicits the *maximal* response to a given pattern is declared as the *winner* for that pattern. The *winner*, then, conditions the plasticity of synapses of neurons which are close to that region of the cortex.

Explicitly, this involves two kinds of lateral control mechanisms [11]: (1) Declaring the neuron that has the best match with the input as the *winner*, based on an activity-dependent competition ('the winner-takes-all' (WTA) mechanism); and (2) Adaptive improvement of the match in the neighborhood of neurons centered on the *winner*. Corresponding to these two processes, two *independent* interaction kernels are defined [11]: (i) *Activation kernel*, usually the "Mexican-hat" function (4), which also controls intra-cortical interaction, and (ii) *Plasticity control kernel* (PCK), which defines the effect of local activity on the learning rate of neurons in its neighborhood, given by (15).

The activation kernel controls *only* the activity or response of the neurons (as in (10)), and helps in declaring the winner. The PCK, on the other hand, is considered to model some kind of diffuse chemical agents or special chemical transmitters of messengers, whose amount in the neighborhood is proportional to local activity. The PCK *does not* control activity but *only* the plasticity (learning rate) in the neighborhood based on (i) local neural activity, and (ii) the distance between the *winner* and the location of the other neuron in the neighborhood [11].

The algorithm for simulation is as follows:

(1) Initialize synaptic weights S^{ON} and S^{OFF} with random strengths uniformly distributed over $(1 \pm S_{noise})A(\mathbf{x} - \alpha)$. $S_{noise} = 0.2$.
(2) Present a sinusoid of randomly chosen frequency, orientation and phase shift as input $\mathrm{Im}(i, j)$ to the ON- and OFF-channel LGN layers. The range of the input frequency is specified, while orientation varies from 0 to 180°, and the phase shift spans the entire 0–2π radians.
(3) Compute the responses of ON- and OFF-center LGN channels as in (6). Compute the cortical responses $O_{\mathrm{c}}(\mathbf{x})\ \forall \mathbf{x} \in \mathscr{C}$ using (10).
(4) Declare neuron at $\mathbf{w}$ to be the *winner* if $O_{\mathrm{c}}(\mathbf{w}) > O_{\mathrm{c}}(\mathbf{y})\ \forall \mathbf{y}(\neq \mathbf{w}) \in \mathscr{C}$. Neurons which have at least 90% of their synapses saturated are not allowed to participate in this competition.
(5) Compute the changes in weights of the *winner* and its neighbor neurons using [2]

$$\Delta S^{\mathrm{ON}}(\mathbf{x}, \alpha)|_U = \eta A(\mathbf{x} - \alpha)\mathscr{K}(\mathbf{x}, \mathbf{w}) \sum_{\beta} [C^{\mathrm{ON,ON}}(\alpha, \beta) S^{\mathrm{ON}}(\mathbf{x}, \beta) + C^{\mathrm{ON,OFF}}(\alpha, \beta) S^{\mathrm{OFF}}(\mathbf{x}, \beta)], \tag{14}$$

where $\mathscr{K}(\mathbf{x}, \mathbf{w})$ represents the *plasticity control kernel* (*PCK*), defining the nature of neuronal plasticity in the *neighborhood* of the *winner* $\mathbf{w}$, based on local activity. The PCK, in our case, is given by

$$\mathscr{K}(\mathbf{x}, \mathbf{w}) = G(\mathbf{x} - \mathbf{w}, \sigma_n), \tag{15}$$

where σ_n, the neighborhood parameter, defines the neighborhood of the *winner*. In this case, the correlation functions are directly obtained from the responses of LGN neurons.

[2] What is given here is the update equation for the ON-channel weights. The OFF-channel equation is also similar to this, with ON and OFF being substituted by OFF and ON, respectively, throughout.

Enforce the zero-sum constraint by subtractive normalization.

Cut off and freeze synapses which have reached either maximum value or zero value. Renormalize the weights to take this change into account.

(6) Repeat *Steps* 2–5 until at least 90% of synapses of *all* the neurons are saturated. This is defined as the *convergence* of the algorithm.

Note that the synapses which are frozen (Step 6) are not allowed to change further. This is achieved by (i) assigning null derivatives to the frozen synapses, and (ii) subtractive normalization and renormalization of weights of only the unfrozen synapses (see [13] for further details).

2.2.3. Numerical results

The algorithm has been implemented in C++, and executed on a SGI Octane workstation. Each iteration takes about 20 s. The number of iterations varies from 20 000 to 150 000, depending upon the choice of parameters. In what follows, unless otherwise specified, the default parameters are as follows: $\eta = 0.001$, $r_I = 0.3$, $S_{\max} = 4.0$. The sinusoids presented as inputs to the model are chosen randomly from $\mathscr{S}(0.4, R, R)$–$\mathscr{S}(0.8, R, R)$. The frequency range is set to 0.4–0.8, taking a cue from the range of frequencies obtained with the output of Miller's algorithm. The default value for the size of both the cortical and LGN arrays is 32×32.

Fig. 4 shows results of typical simulations obtained with various random initializations of the algorithm. The neighborhood parameter σ_n is set at 4.0 for the simulations. The preference maps in Fig. 4 show that the organization is highly dependent upon the initialization process (*Step* 1 of the above algorithm). Observations from the results by varying σ_n (also analyzed in Section 3.1, below) show that the properties of cortical maps listed at the end of Section 3.1 hold for the maps obtained with such random initializations also. The only difference lies in the case where the PCK is a delta function; in this case, since the initialization is random, the organization of preferences is also random.

An important observation is that the iso-orientation domains increase in size with increase in σ_n. This is expected because as σ_n increases, the number of neighboring

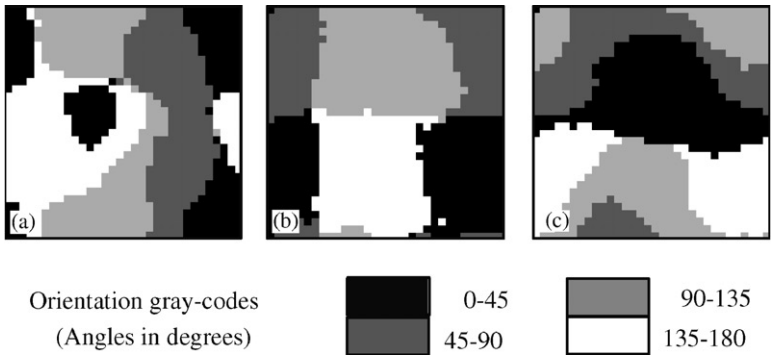

Fig. 4. Preference maps with various random initializations to the proposed dynamics.

neurons and the degree of co-operation among them also increase, leading to continuity in preferences. This may also be interpreted as follows: σ_n controls the width of the hypercolumns.

3. Development under normal rearing

A well-known hypothesis concerning the development of orientation-selectivity is the following [1,5,13–18]:

Hypothesis A: Endogenous, spontaneous neural activity plays a prominent role in the *establishment* of orientation selectivity and columnar organization of orientation selective simple cells. Building upon this *initial* selectivity, visual experience, post-natally, *can* 'actively' modify the characteristics of receptive fields and the preference organization.

In other words, the 'main' determinant of development during the stage before eye-opening is the *spontaneous neural activity*, while that during the stage after eye-opening is the *visual experience*. Further, it is also known from these studies that visual experience is an essential component for normal development and maturity of orientation selectivity, and that sharpening of selectivity is observed with normal development [8,15,18].

In an attempt to quantify Hypothesis A, and to provide a *basic* insight into the combined pre- and post-natal development regimes, we propose to initialize the algorithm in Section 2.2.2 with *maturing* weights from Miller's simulation. Explicitly, we *interpret* such an initialization to quantify the two stages of development as follows:

- *Before eye-opening*: Spontaneous neural activity plays a crucial role in the development. The correlations among the LGN channels are modelled as DoG functions, and the update equation is given by (13). The simulation runs until $\mathscr{P}$% of the synapses saturate. (This may be contrasted with Miller's algorithm where convergence is defined at the point where 90% of the synapses saturate.) In the sequel, this stage will be referred to as the DBEO (development before eye-opening).
- *After eye-opening*: Neural responses to the visual environment play crucial roles in the developmental process. The neurons, which already have a *crude* selectivity and a basic organization (as a result of development in the previous stage), are allowed to be driven by sinusoidal gratings of varied orientations, frequencies and phases. The algorithm given in Section 2.2.2 guides the developmental process. In the sequel, this stage will be referred to as the DAEO (development after eye-opening) stage.

Such a quantification provides the framework for (i) analyzing the effect of the initial RF profile and organization on the mature selectivity and organization (i.e., studying the relative roles of activity and experience on RF development); (ii) quantifying physiological parameters like (a) the critical period and (b) the time of onset of visual experience, and (iii) analyzing the effects of biased visual environments. However, such an interpretation is not exempt from technical problems, some of which are listed below:

(a) *Why should we use sinusoids*? If the model is to unify pre- and post-natal environments, then it would be more appropriate if natural images are considered.

Sinusoids cannot represent broad-band signals characteristic of natural images. Therefore, how can visual experience be analyzed with sinusoids? Some reasons for the choice of sinusoids are as follows:

(1) *Incompleteness of the model*: The model neither takes into account the vertical dimension of the cortex (along which RF sizes are supposed to vary) nor does it consider a dynamic arbor diameter. Hence, there is no way by which RF of multiple sizes (needed to represent natural images) can be formalized. Therefore, we borrow a cue from Miller's simulation results, and choose sinusoidal gratings which can be *accommodated* within the given arbor diameter.
(2) *Control of the input*: Sinusoids offer ultimate control of variables like orientations and spatial frequencies fed as input to the model. This is helpful when the model is to be tested with biases in the input environment (Section 5).

(b) *Why should there be a change in plasticity rules and mode of update during DBEO and DAEO stages*? A plausible reason is the relative variation in the response levels of neurons between the DBEO and DAEO stages. In the DBEO stage, the spontaneous neural activity of the neurons would all have the same order of magnitude, and hence the chemicals guiding the plasticity would be *unbiased*. However, during the DAEO stage, the neuron which exhibits a *higher* response to a presented input expresses a relatively prominent activity. If we consider the effect of trophic factors to be dependent on activity [1,11], then the changes in synaptic efficacy would be concentrated in the neighborhood of the *winner* (also see end of Section 2.2.1). In other words, the change in the order of relative responses drives the change in plasticity dynamics.

With these problems of interpretation in the background, we now proceed to the simulation. The first step involves the simulation of the DBEO phase. Synaptic values corresponding to various percentages of synaptic saturation in this phase are stored. This set of synapses is employed as the *base configuration* for the next (DAEO) phase of the simulation. The parameters chosen for the DBEO phase are: $\eta = 0.001$, $r_C = 0.25$, $r_I = 0.3$, $S_{\max} = 4.0$ [13]. The parameters for the DAEO phase are as given in Section 2.2.3. Further, $\mathscr{P} = 35\%$ unless otherwise specified.

3.1. Variations in the PCK

In this section we present results corresponding to variations in the parameter regime of the PCK. We consider three cases:

(1) δ-function as the PCK.
(2) Gaussian PCK with constant neighborhood.
(3) Gaussian PCK with a tapering neighborhood.

Case 1: Let us initially assume that the *winner* of the competition (Section 2.2.2) is the *only* neuron to get updated; in other words, the function $\mathscr{K}(\mathbf{x}, \mathbf{w})$ in (14) is a δ function, which is 1 for the *winner*, and 0 for the other neurons—this is the limiting case of a Gaussian with $\sigma_n \to 0$. By definition, only a sinusoid with characteristics (i.e., orientation, frequency and phase) similar to those of the neuron's RF will elicit maximal

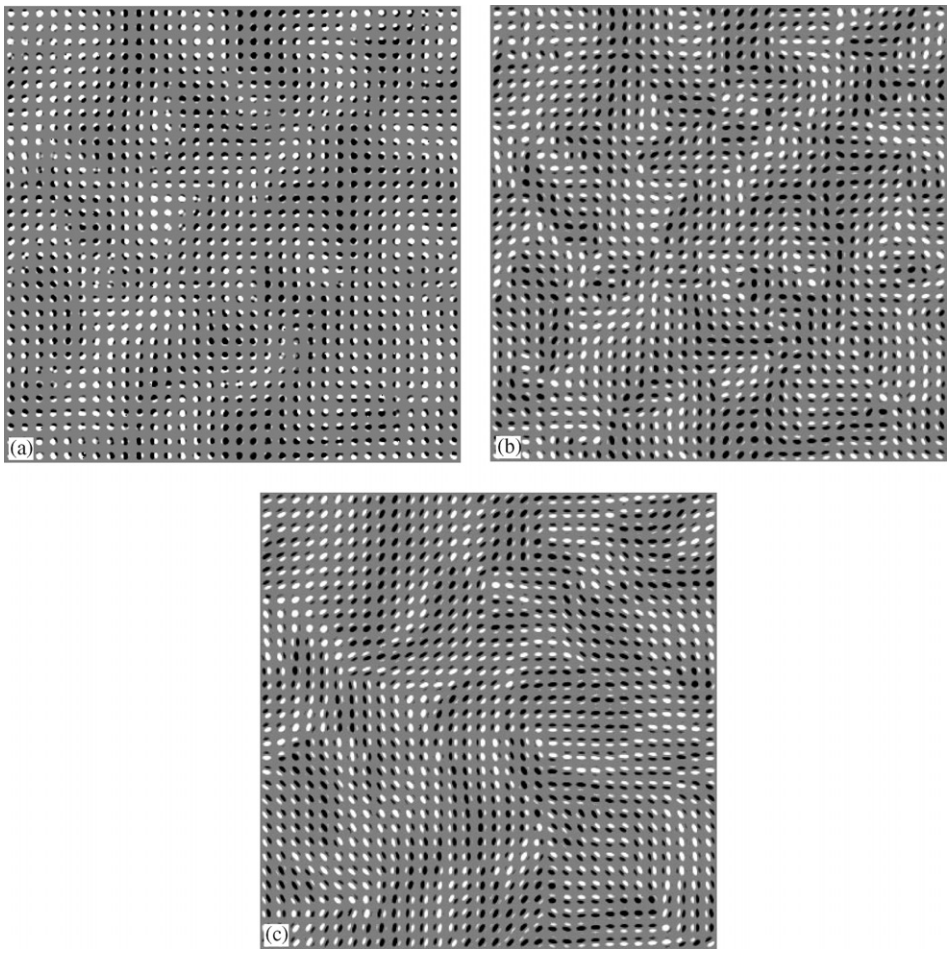

Fig. 5. (a) RF profiles with Miller's algorithm. (b) RF profiles built on developing RF profiles from Miller's algorithm with a delta function as PCK, using the proposed plasticity rule. (c) RF profiles built on developing RF profiles from Miller's algorithm with $\sigma_n^{\mathrm{i}} = 3.0$, $\sigma_n^{\mathrm{f}} = 1.0$.

response from it. This, along with a δ function as the PCK, ensures that a neuron will be updated *only* with respect to sinusoids with similar characteristics. Hence, the preferences of the cells do not change *significantly* (from the base configuration) during simulation.

And this may be observed from Fig. 5 in which Fig. 5(a) shows the RF profile corresponding to Miller's algorithm ($r_C = 0.25$, $D_A = 13$ and $\gamma_C = 3$), and Fig. 5(b) corresponds to the profile built on a developing array (based upon Miller's simulation with $\mathscr{P} = 35$) with a δ-function as the PCK. It is seen that the preferences of the cells in Fig. 5(b) have not changed *significantly* with respect to those in Fig. 5(a). A quantitative analysis shows that the mean difference in orientation

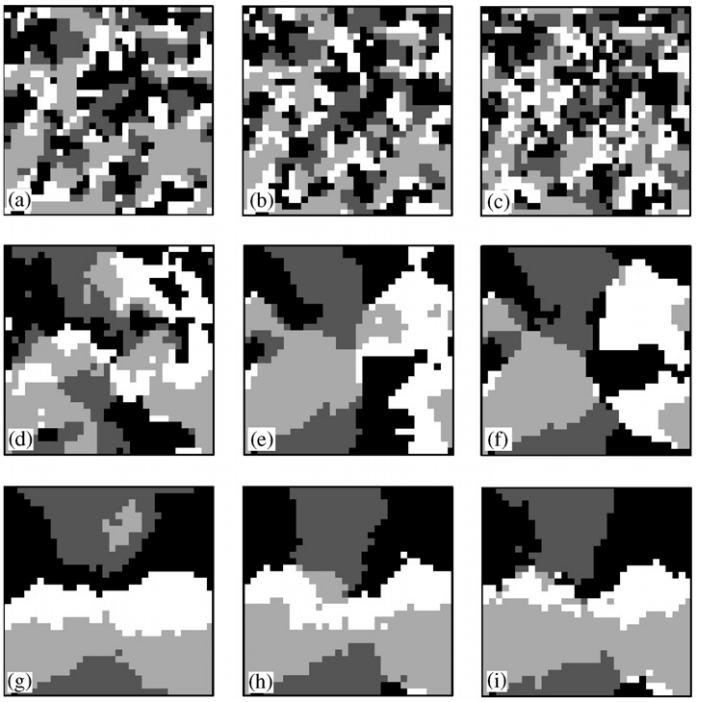

Fig. 6. Effect of the neighborhood parameter, σ_n, on the organization of orientation preferences of the model neurons: (a) Organization with Miller's algorithm (b) Organization with 35% of synapses saturated in DBEO phase (c) $\sigma_n = 0.5$, (d) $\sigma_n = 1.0$, (e) $\sigma_n = 2.0$, (f) $\sigma_n = 3.0$, (g) $\sigma_n = 4.0$, (h) $\sigma_n = 6.0$, (i) $\sigma_n = 9.0$.

preferences of cells is less than 15°. It may also be observed that the RF profiles are sharpened. Quantitatively, the MDOS for the model cells shown in Fig. 5(b) is 0.232 ($\min = 0.00142, \max = 0.3211$). In comparison, the MDOS for the cells in Fig. 5(a) is 0.1809 ($\min = 1.68775 \times 10^{-17}$, $\max = 0.318305$). The numbers are comparable in magnitude (and order) to the results in [13].

Case 2: As a next step, we set the PCK as given by (15), and fix σ_n as a constant throughout the simulation. It is observed that the organization of cell preferences undergoes considerable changes with variation in σ_n. Fig. 6 establishes the changes that occur by varying σ_n. Fig. 6(a) shows the organization of the orientation preferences of the model neurons with Miller's algorithm. Fig. 6(b) presents the organization of orientation preferences of the *base configuration* (i.e., at the moment of onset of the DAEO phase with $\mathscr{P} = 35\%$). These may be compared with the organizations of the orientation preferences obtained with simulations run with different values of σ_n (Fig. 6(c)–(i)).

Observations from the simulations and the figures indicate the following: (i) the organization (of the orientation preferences) tends towards the organization of Fig. 6(b) as σ_n *tends* towards zero, (ii) convergence of the algorithm is delayed as σ_n decreases (number of iterations is 128 085 for $\sigma_n = 0.5$, and 2224 for $\sigma_n = 9.0$), and

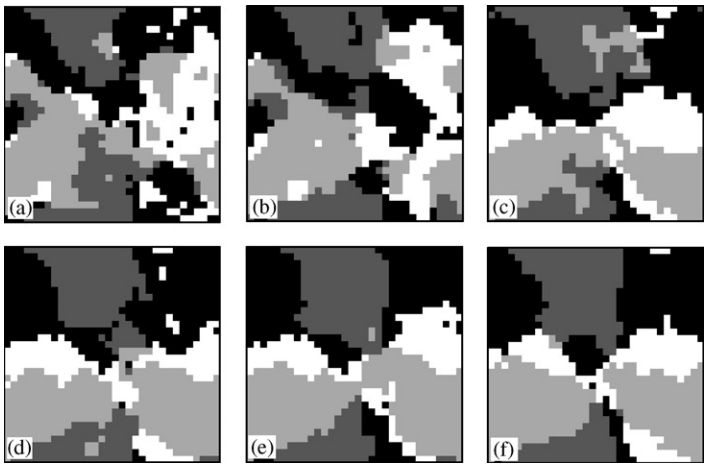

Fig. 7. Organization of orientation preferences with $\sigma_n^{\mathrm{f}} = 1.0$ and (a) $\sigma_n^{\mathrm{i}} = 2.0$, (b) $\sigma_n^{\mathrm{i}} = 3.0$, (c) $\sigma_n^{\mathrm{i}} = 4.0$, (d) $\sigma_n^{\mathrm{i}} = 5.0$, (e) $\sigma_n^{\mathrm{i}} = 6.0$, (f) $\sigma_n^{\mathrm{i}} = 9.0$.

(iii) the size of iso-orientation domains increases with increase in σ_n. While the first observation implies that this case is more general than the previous one, the second and third observations show the importance of updating the neighboring neurons along with the *winner*.

Case 3: Here, we consider an update mechanism with a tapering neighborhood [11]. To be more precise, we set the initial value of σ_n (denoted by σ_n^{i}) to be initially high, and reduce it slowly (to σ_n^{f}) as simulation proceeds. To this end, we employ a *development-regulated* paradigm, i.e., σ_n is assigned to σ_n^{i} initially, and for every 10% increase in the percentage of the total saturated synapses, σ_n is divided by 2. This is continued until σ_n reaches σ_n^{f}, after which it is set to σ_n^{f}.

Fig. 7 demonstrates the effect of σ_n^{i} on the organization. Note that σ_n^{f} is set at 1.0 for all these cases. (See Fig. 6(d) for the case, $\sigma_n^{\mathrm{i}} = \sigma_n^{\mathrm{f}} = 1.0$.) Typical RF profiles obtained with such a simulation are presented in Fig. 5(c) ($\sigma_n^{\mathrm{i}} = 3.0$, $\sigma_n^{\mathrm{f}} = 1.0$). This may be compared with Fig. 5(a) and (b) (cf. Case 1, above). An analysis of the results leads to the following observations (cf. Figs. 6 and 7 also):

- Degree of selectivity is sharpened. Quantitatively, the MDOS for the model cells shown in Fig. 5(c) is 0.2654 ($\min = 0.00142, \max = 0.3410$). In comparison, the MDOS for the cells in Fig. 5(a) is 0.1809 ($\min = 1.68775 \times 10^{-17}$, $\max = 0.318305$).
- The organization of orientation preferences has changed considerably, and structures exhibiting singularities have emerged.
- The corresponding Fourier power spectra of the maps obtained indicate that some of them are bandpass in nature (like Fig. 6(d) where typical *linear zones*[3] are visible), whereas others have typical low frequency modes.

[3] Linear zones in a orientation map are those where iso-orientation regions are organized in parallel slabs.

- The nearby cortical cells prefer stimuli with similar orientation except for singularity lines across which orientation preference reverses/changes.
- The spatial phase of receptive fields gradually shifts.
- The sizes of iso-orientation domains increase with increase in σ_n (cf. Fig. 5).
- There is no change in MDOS with changes in σ_n.

Considering that the iso-orientation domains increase in size with σ_n, it is essential to take into account its values for the interpretation—see the beginning of Section 3—of combined pre-natal–post-natal development in order to *conform to* biological realities. It is known that the normal (i.e., without any biases in the environment) post-natal variations in the organization of orientation preferences are minimal (see [5,3,8]). Therefore, σ_n has to be *low*; however, the exact values of σ_n^{f} and σ_n^{i} should depend on experimental considerations. It may be noted here that the (extreme) case where σ_n tends to zero (in the limiting sense)—the case where the PCK is set to be the δ-function—sharpens *only* the selectivity of the cells, and *does not* change the organization of preferences from the one with which it was initialized (Fig. 5(b)).

3.2. Onset of visual experience

The onset of the DAEO phase characterizes eye-opening and the onset of visual experience. (It is a general assumption that eye-opening marks the onset of visual experience.) However, recently, there have been questions on this basic assumption. The authors of [12] raise the following question: Do visual stimuli presented through closed eye-lids *before eye-opening* drive neuronal activity in LGN and in the PVC of the cortex? In the attempt to answer the question, they demonstrate experimentally that such stimuli *can* drive neuronal activity and that the selectivity of cortical neurons to the orientation of gratings presented through the closed eyelids *improves* with age [12]. This raises the question of whether eye-opening *really* marks the onset of visual experience and of whether visual experience starts well before eye-opening. However, White et al. [18], referring to this possibility, observe that ([18, p. 1049]):

> Although cortical responses can be evoked through naturally closed eyelids in very young ferrets (post-natal weeks 4–5) [12], our results indicate that the contribution of visual experience to the maturation of orientation selectivity is confined to the developmental period that follows eye opening.

Further, they observe that lid suture has devastating effects on the maturation of orientation selectivity, as opposed to dark rearing, where the effects are more 'modest'. Owing to this discrepancy in views, we, in this paper, have used 'eye-opening' and 'onset of visual experience' interchangeably. The exact time of the onset of visual experience is quantified in the model by $\mathscr{P}$ that determines the exact nature of the base on which the DAEO is to be built. In other words, it quantifies the balance between spontaneous activity and visual experience, and decides the effect of the former on the mature organization and selectivity behavior of model cells. In order to study the effect of the onset of DAEO, simulations of the DAEO phase were run with different *base configurations* corresponding to various values of $\mathscr{P}$. The neighborhood parameters

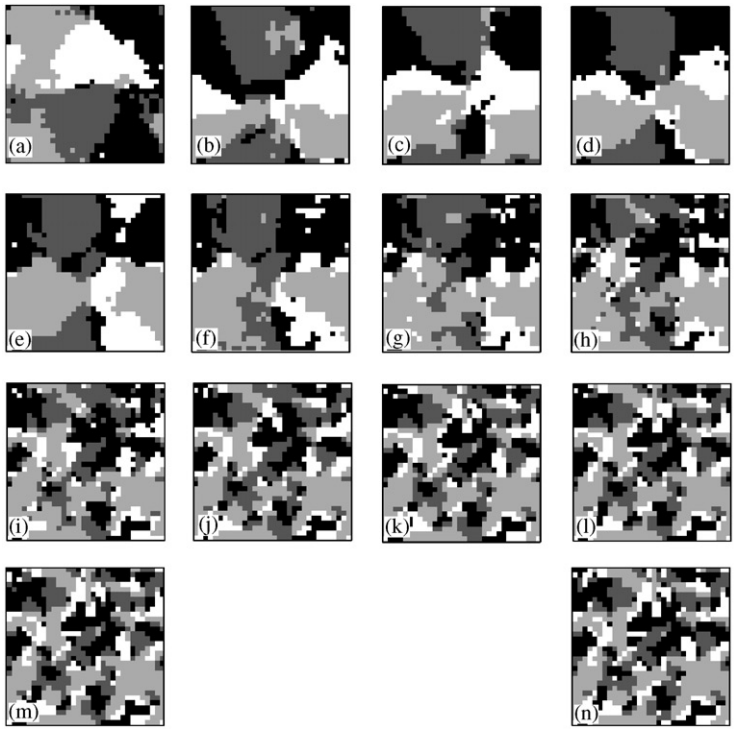

Fig. 8. Effect of the onset of DAEO on the organization of orientation preferences: (a) $\mathscr{P}=0\%$, (b) $\mathscr{P}=5\%$, (c) $\mathscr{P}=20\%$, (d) $\mathscr{P}=35\%$, (e) $\mathscr{P}=45\%$, (f) $\mathscr{P}=55\%$, (g) $\mathscr{P}=65\%$, (h) $\mathscr{P}=70\%$, (i) $\mathscr{P}=75\%$, (j) $\mathscr{P}=80\%$, (k) $\mathscr{P}=82\%$, (l) $\mathscr{P}=85\%$, (m) $\mathscr{P}=87\%$, (n) Organization with Miller's algorithm.

employed for the simulations are: $\sigma_n^{\mathrm{i}}=6.0$, $\sigma_n^{\mathrm{f}}=1.0$. The number of iterations required for the convergence decreases with an increase in $\mathscr{P}$.

The onset of DAEO affects both the receptive field properties and the organization of orientation preferences of the neurons. The effect of $\mathscr{P}$ on the organization of orientation preferences of model neurons is brought out in Fig. 8. Whereas Fig. 8(a)–(m) illustrate the changes that the organization undergoes for various $\mathscr{P}$'s, Fig. 8(n) presents, *for comparison*, the organization obtained from employing Miller's algorithm (i.e., $\mathscr{P}=90$).

It may be noticed from Fig. 8 that the organization tends towards that of Miller's as $\mathscr{P}$ increases. This is because an increase in $\mathscr{P}$ allows the number of frozen synapses also to increase, thus resisting further changes. In other words, at later stages, the cells become committed, and lose their ability to *alter* themselves in a manner determined by the environment. The effect of such a commitment may also be observed from the significant difference between Fig. 8(a) and (b), in marked contrast with the gradual change from Fig. 8(b) to (m). More specifically, the difference between the cases, (i) $\mathscr{P}=0$, where spontaneous activity plays *no* role; and (ii) $\mathscr{P}=5$, where its role is minimal, is prominently observable. This shows that even a minimal influence of the

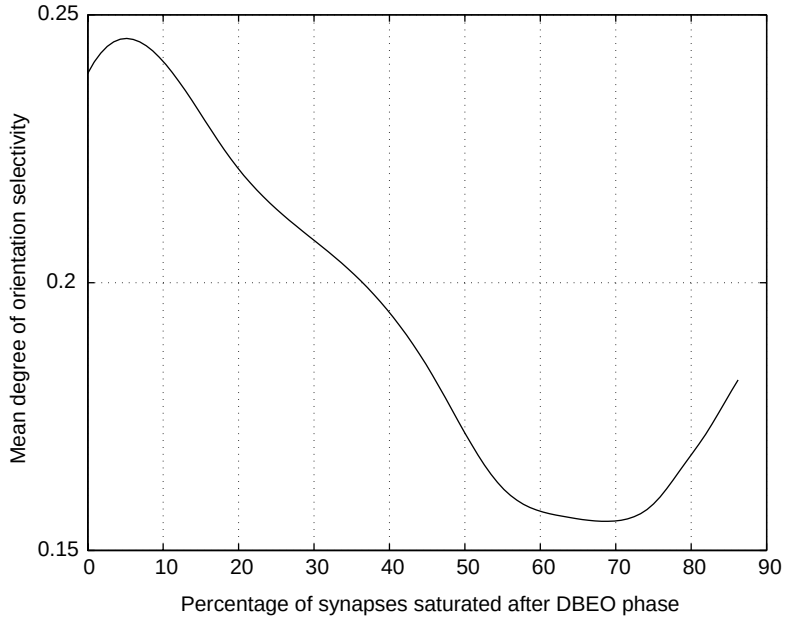

Fig. 9. Graph illustrating the effect of the onset of the DAEO phase on the mean degree of orientation selectivity of the model neurons.

DBEO phase can affect the WTA process, and modulate the organization in the DAEO phase.

The parameter $\mathscr{P}$ also has a significant effect on the degree of orientation selectivity of the model neurons. This may be seen from Fig. 9, which illustrates, graphically, the effect of $\mathscr{P}$ on the MDOS of the neurons. It is observed that the MDOS initially decreases, saturates, and then increases with an increase in $\mathscr{P}$. The left end of the graph indicates a complete DAEO simulation whereas the right end corresponds to a complete DBEO simulation. From the graph, it can be inferred that the DAEO phase of algorithm *inherently* yields RFs of higher degree of orientation selectivity. However, as the commitment of the cells to particular orientations increases with increase in $\mathscr{P}$, the possibility that the preference behavior of the *winner* neuron does not have exact correspondence with the input grating *also* increases. This, in turn, leads to *anomalous* synaptic updates in the *winner* and its neighbors, thereby affecting the proper formation and elongation of the subregions, and leading to a reduction in the degree of orientation selectivity.

The increase in MDOS at the tail-right-end of the graph may be attributed to the *complete* commitment of the neurons to orientations, corresponding to those obtained from the base DBEO configurations. This reduces the possibility of any further modification in synaptic weights, thereby leading to a convergence towards the DBEO selectivity behavior. It has to be noted here that the MDOS corresponding to a complete DBEO simulation (i.e., Miller's algorithm, $\mathscr{P} = 90$) is 0.1809 (*with*

min $= 1.68775 \times 10^{-17}$, max $= 0.318305$—see Fig. 5(a), Section 2.2) which matches with the last value in the graph ($\mathscr{P}=86.2206$, MDOS$=0.180834$). Further, the difference between the cases, (i) $\mathscr{P}=0$ and (ii) $\mathscr{P}=5$, may also be noted.

4. Critical period and dark rearing

The early post-natal period, during which the development of a neural function (e.g., orientation selectivity, ocular dominance, direction selectivity) is susceptible to biased environments, is called the *critical period* of that function. The *main contribution* of the present paper is believed to be the result that the proposed model quantifies the developmental aspects of oriented receptive fields in a combined pre-natal–post-natal environment. While attempting to substantiate this result, we need to answer the following questions that arise naturally: How does the model quantify critical period? Can the model explain the phenomenon associated with critical period of neurons that exhibit orientation selectivity?

It turns out, from the model formulation (Section 2), that the model *does indeed* quantify the critical period phenomenon. In order to be explicit, we characterize the biological critical period phenomenon as follows:

(a) It is the period during which a change in the system is possible. As the system tends closer to the end of the critical period, the extent of possible changes reduces.
(b) Though the molecular basis for critical periods is not yet clear, it is known that the following factors play crucial roles in determining the span of the critical period: (i) sensory experience, (ii) NMDA (N-Methyl-D-Aspartate) receptors, (iii) neurotrophins and (iv) inhibitory circuitry [1]. Among these, neurotrophins are the only factors for which a causal link between expression of a single molecule and duration of the critical period has been established (see [1] and the references therein). It is also known that these molecules are developmentally regulated and activity-dependent [1].

Analyzing the model from this *perspective*, we find that, in our model,

(a) the process of synaptic saturation quantifies the duration of the critical period. The higher the percentage of synapses saturated, the closer the system is to the *end* of its critical period. The *end* of the critical period is quantified in our case as the saturation of 90% of synapses in *each* neuron individually. Explicitly, as the system tends towards 90% synaptic saturation, the amount of changes it can undergo reduces, thus signalling the end of the critical period.
(b) the neighborhood parameter σ_n is a *development-regulated* (dependent on the current percentage of synaptic saturation) and *activity-dependent* (it controls the synaptic update of neurons only around the winner, which is the centre of the activity bubble) parameter. This may be viewed as a *simple* model for the *developmentally regulated* molecules (like the NMDA receptors and the neurotrophins, cf. physiological interpretation of the neighborhood parameter in [11]) and/or convergence of axons. It may also be noted here that, like these molecules,

the parameter σ_n also controls the duration of the *critical period* by prolonging or cutting short the duration for the convergence of the algorithm (see Section 3.1).

Against this background of the quantification of critical period and parameters associated with it, we now analyze the implicit/explicit hypotheses associated with such an interpretation, and bring out the biological meanings of the various experiments conducted on the model. The relevance of the outcomes of such experiments with reference to biological realities is also discussed. Explicity, we analyze (i) the convergence criteria and its association with this interpretation of critical period, and (ii) the outcomes of subjecting the model to dark rearing.

4.1. Convergence criteria and critical period

The convergence criteria for the algorithm require that *all* the neurons in the model have to reach 90% synaptic saturation. Further, the process of winner selection *does not* allow any neuron which has reached 90% of synaptic saturation to compete. These, when translated to biology, lead to the following *implicit* hypothesis:

Hypothesis B: Individual neurons, based upon the local concentration of certain chemicals, have their own critical periods.

Explicitly, according to the algorithm, some neurons may reach their 90% target before other neurons. This is dependent on various factors like (a) initial distribution of weights, (b) the order in which sinusoidal gratings are presented to the system, and (c) the value of σ_n which controls the extent (in the cortex) to which an update *spreads*. This, in turn, implies that some neurons have reached their convergence—that is, in the light of the above discussions, reached the end of their critical period—before others have. In other words, the neurons which have *converged* have crossed their critical period, and, as a consequence of having lost their ability to change according to the environment, are not part of the competition. This, in turn, means that some neurons have still not reached their critical period while others have, and are still amenable to changes, thereby showing the localized nature of critical periods in the model. On the validity and consequences of the hypothesis, the following may be noted [1]:

- Neurotrophins guide the duration of critical periods, and have activity-dependent behavior
- Activity is localized, in the sense that only cells which correspond to a given orientation and spatial frequency at a given retinotopic position fire vigorously.

When we combine the above ideas, we arrive at Hypothesis B. It is interesting to note that the development of ocular dominance columns has been modelled by taking into account the competition for neurotrophic factors. In this context, see [9] in which the authors propose a model where each cortical cell has a fixed pool of trophic factors to distribute over all its thalamic inputs, with each individual connection having a fixed amount of material for *improving* its connection strength. Most importantly, they show that ocular dominance column development is prevented in a *local neighborhood* where neurotrophin concentration is in excess [9]. They also discuss the biological plausibility of their model. In fact, *hypothesis B* is an extension of this localized

behavior of neurotrophins with respect to orientation selectivity. We also discuss the implications of this hypothesis when we discuss the results of selective rearing (see Section 5.5 below).

4.2. Dark rearing

Dark rearing, biologically, corresponds to rearing an animal without visual experience till the end of the critical period of the given function. Within the framework of our model, the experiments conducted with respect to variation in $\mathscr{P}$ may be viewed as follows: the animal is subjected to *dark rearing* for a certain period of time (within the critical period) and, then, is allowed to gain visual experience. The exact period is determined by the value of $\mathscr{P}$. If $\mathscr{P}$ is low, then the model accommodates itself to the environment, improves its selectivity behavior (cf. Section 3.2), and goes through the normal developmental course, conforming to the outcomes of dark rearing in animals [19].

However, in case of the absence of visual experience during the entire critical period, (i.e., the case where $\mathscr{P}$ is set at 90), the developmental process is *entirely* driven only by spontaneous neural activity (or, more appropriately, *dark activity*). This leads to receptive fields and a preference organization similar to those of Miller's algorithm. This, in turn, indicates that dark rearing, within the model framework, *freezes* the degree of orientation selectivity (i.e., the sharpening does not extend beyond Miller's limits). This should be contrasted with the biological fact that orientation selectivity deteriorates if the eyes are not allowed to open [8]. The model *does not* predict a deterioration because we assume that dark activity continues to drive orientation selectivity (cf. [2,3]), which, in our model, effectively leads to Miller's analysis.

Summarizing the results of subjecting the model to dark rearing, we see that:

- If the model is subjected to dark rearing for a short duration, and then is allowed to be visually driven, orientation selectivity improves indicating an accommodation to the visual environment. The amount of increase in selectivity, however, decreases with an increase in the duration of dark rearing (cf. Section 3.2). This is consistent with biological findings.
- In the limiting case, where the model is subjected to dark rearing till the end of the critical period, the model converges to Miller's algorithm. This implies a freeze, and *not* a deterioration in the orientation selectivity as, in fact, biology predicts [8].

Hence, the model *partially* conforms to biological realities in the case of dark rearing. This shows there do exist other parameters, which are not considered in the model, that control the post-natal developmental stage.

5. Selective rearing

It has been shown (see [15] and the references therein) that animals reared in biased visual environments (i.e., environments primarily made of a single grating with a given spatial frequency and orientation) during their *critical period* display a number of

defects in their behavior. The defects include jerky head movements and inability to estimate the depth of objects. More importantly, most of the cells in such animals respond, primarily, to orientations they were reared with. This is in stark contrast with those orientations to which the animals were not exposed, for which the corresponding cortical areas are relatively smaller [15].

The analysis of the effects of biases on the model performance would require varying the input grating statistics. In this section, we analyze the effects of variations in input grating parameters. The results are presented corresponding to (a) variations in the orientations (parameters θ_h and θ_l), and (b) variations in the frequency of sinusoidal gratings (parameters ω_h and ω_l). In what follows, we analyze the model with $\mathscr{P} = 0$. The analysis on the behavior of the model with variation in $\mathscr{P}$ is presented later (Section 5.3).

5.1. Variations in input orientations

The range of orientations presented to the model has a direct effect on the range of orientations the model neurons respond optimally to. This conclusion is arrived at on the basis of two experiments: (i) the model is presented with sinusoids of single orientation (i.e., $\theta_h = \theta_l$); and (ii) the model is presented with a *limited* range of orientation. Nevertheless, in both the cases, the sinusoids are allowed to vary in frequency and spatial phase.

In the first experiment, all the model neurons develop in order to respond optimally only to the input orientation. Quantitatively, the preferred orientation of the cells has a 3° variance with respect to the reared oriented. In the second experiment, where the model is presented with only a *limited range* of input orientations, it is observed that the neurons also *tune* themselves only to the chosen *limited range* of orientations.

5.2. Variations in grating frequency range

In order to assess the effects of variations in input grating frequency, simulations of the model are carried out with gratings of varied orientations and spatial phase, but with a single spatial frequency ($\omega_h = \omega_l$). Such simulations indicate that the organization of the preferences and the number of iterations for the algorithm to *converge* do not undergo major changes due to variation in the frequency range. However, significant changes are observed in the receptive field properties of the model neurons.

It is observed, from the developed receptive fields profiles corresponding to various input frequency ranges, that, as the input frequency increases, the number of ON and OFF subregions within a receptive field increases. This is to be expected because receptive fields require to have *thinner* ON/OFF subregions for being optimally selective to higher frequencies. In addition to this, the fixed size of the receptive fields (by the arbor function) also contributes to the increase in this number of subregions. This effect of frequency variation on the subregions is shown in Fig. 10. This also implies that the range of spatial frequencies to which the model neurons optimally respond varies. When rearing is done with only one spatial frequency, the resulting neurons *tune* themselves to frequencies around it (quantitatively, around 0.05 radians

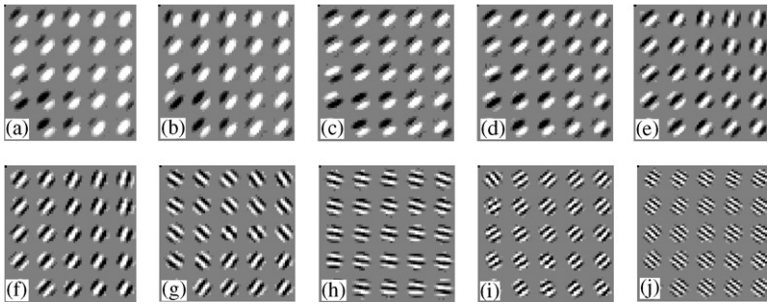

Fig. 10. Typical RF profiles of model neurons obtained with various input spatial frequencies: (a) $\omega = 0.55$ radians, (b) $\omega = 0.6$ radians, (c) $\omega = 0.7$ radians, (d) $\omega = 0.8$ radians, (e) $\omega = 1.0$ radians, (f) $\omega = 1.25$ radians, (g) $\omega = 1.5$ radians, (h) $\omega = 1.75$ radians, (i) $\omega = 2.0$ radians, (j) $\omega = 2.5$ radians.

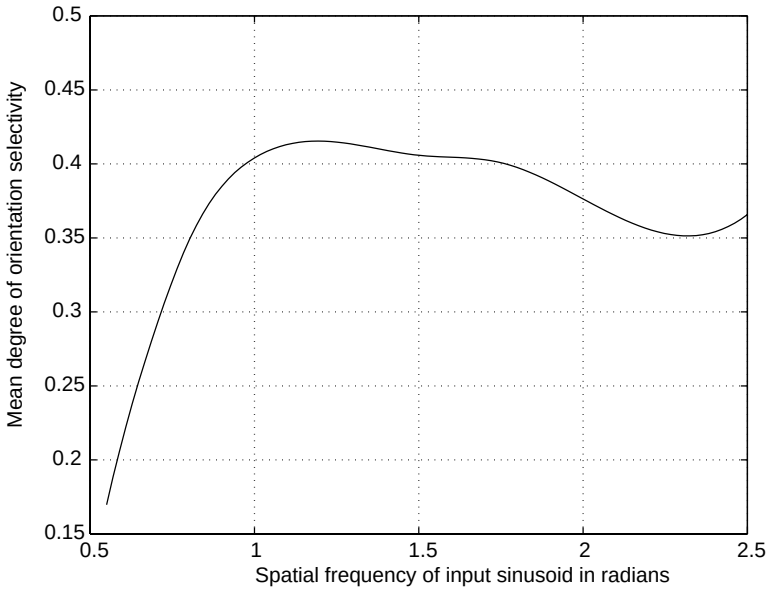

Fig. 11. Effect of input spatial frequency on the degree of orientation selectivity.

with a Gaussian-like distribution with mean at the input frequency). In other words, *the statistics of the preferred frequency range are reflective of those of the reared frequency range.*

Apart from these, any change in the rearing frequency also has a significant impact on the degree of orientation selectivity of the model neurons. This may be seen from Fig. 11. It is observed from the figure that the degree of orientation selectivity increases with an increase in ω until a point where it more or less saturates. This is because of the way in which the orientation selectivity is calculated. Explicitly, as the size of the subregions (ON and OFF) reduces, the amount of overlap between a RF of a given

orientation and the one with a sinusoid of a different orientation reduces. This implies that the response of the neuron, as defined in [13], for the orientation of its RF will be significantly higher than that of the other orientations, leading to an increase in the optimal response frequency of the cell. This, in turn, yields a higher estimate of the degree of orientation selectivity.

5.3. Effect of $\mathscr{P}$

As we had mentioned earlier, the above experiments are conducted with $\mathscr{P}$ set at zero. However, it is observed that, the parameter $\mathscr{P}$ plays a prominent role in determining the amount of variations that the preference statistics can undergo with changes in input. Explicitly, in both the cases of frequency and orientation biases, it is observed that, if $\mathscr{P}$ increases, the effect of biases decreases. This is because, with an increase in $\mathscr{P}$, the number of frozen synapses (at the onset of DAEO) increases, thus resisting further changes. So, the preference statistics follow the input-grating statistics, subject to the constraints in the form of commitments made to the pre-natal preferences (cf. [15]). We will see, in what follows, that $\mathscr{P}$ quantifies the relative rigidity of cortical RFs and maps in a selective rearing environment.

5.4. Quantification of the onset of visual experience

Sengpiel et al. [15] observe that even in animals reared with single orientation, more than one-half of the visual cortex responds best to orientations never 'seen' by the animal. This can be explained within the framework of our model as follows:

Such a representation is due to a delicate balance between spontaneous activity and visual experience (cf. [15]). The parameter $\mathscr{P}$, which controls the relative effects of spontaneous activity and visual experience, controls the amount of cortical area occupied by unseen orientations. Explicity, as $\mathscr{P}$ increases, the neurons get committed to a particular orientation (arising due to spontaneous activity-dependent establishment), and cannot adapt themselves to the environment (cf. Section 3.2). As a consequence, in spite of being subjected to visual inputs of a single orientation, there will be a large set of neurons which respond to other orientations also. This may be observed from Figs. 12 and 13.

Fig. 12 shows the orientation histograms[4] corresponding to various values of $\mathscr{P}$ in a normal rearing environment (made of all orientations and spatial frequencies). It is observed that $\mathscr{P}$—or correspondingly the onset of visual experience—does not have any effect on the distribution of cortical space across the various orientations. The distribution of cortical space is uniform, reflective of the unbiased nature of the environment. The parameters involved are the same as those in selective rearing (given below), the only difference being in the sinusoids presented to the model: $\mathscr{S}(0.4, R, R)$–$\mathscr{S}(0.8, R, R)$. This spans the entire spectrum of orientations.

[4] Orientation histograms are defined as those which depict the percentage of cortical space occupied by cells maximally responding to a given set of orientations.

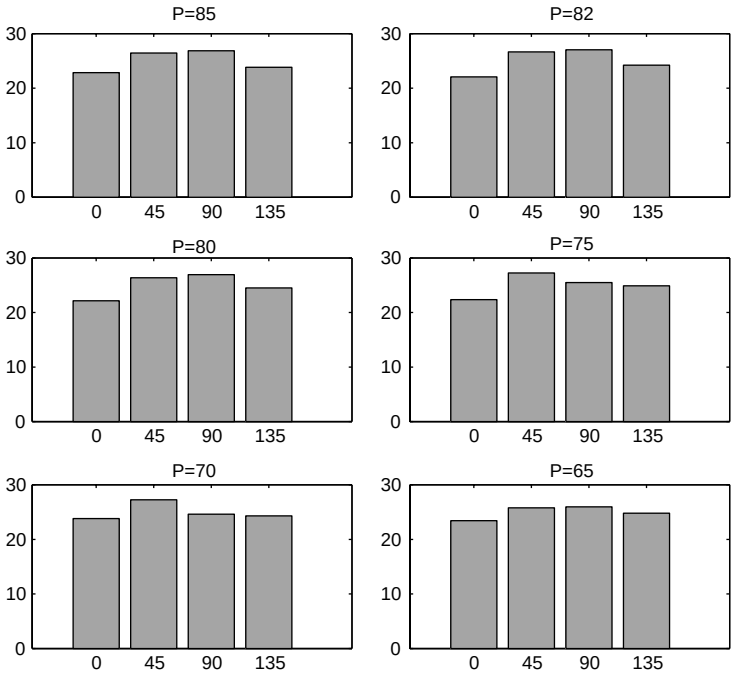

Fig. 12. Effect of $\mathscr{P}$ on the percentage of cortical area occupied by individual orientations $(0°, 45°, 90°, 135°)$ with normal rearing.

These results may be contrasted with Fig. 13 which shows the orientation histograms corresponding to various values of $\mathscr{P}$ in a biased environment. The parameters (of the DAEO phase of the algorithm) for such selective rearing and the reasons for their selection are as follows:

- $\theta_h = \theta_l = 135°$. This is the rearing orientation, chosen randomly.
- $\omega_h = \omega_l = 0.65$. Selective rearing requires that the system is fed with a grating of a single orientation and single frequency. We set this parameter as the frequency of the sinusoid whose zero-crossings match those of the intra-channel correlation function C^{tt}. Incidentally, this is the same technique that Miller [13] employs for estimating the mean preference frequency of the model cells.
- The PCK is chosen as a delta function (cf. Section 3.1) in order to allow only the winner to get updated for a given sinusoid. This, in turn, supports the biological finding that there is little or no change in the preference maps postnatally in a normal rearing environment [3,5].
- Other parameters: Learning rate parameter $\eta = 0.001$, intracortical interaction parameter $r_I = 0.3$ and the maximum value that any synapse can take $S_{max} = 4.0$. Cortical size $= 32 \times 32$.

It is observed from the figure that, with selective rearing, the cortical area occupied by the reared orientation increases with a decrease in the value of $\mathscr{P}$. In other words, the

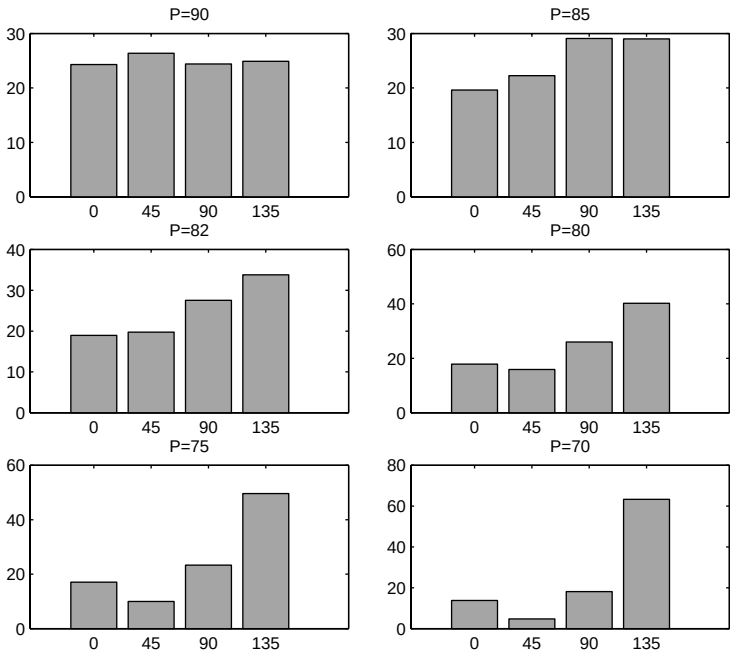

Fig. 13. Effect of $\mathscr{P}$ on the percentage of cortical area occupied by individual orientations $(0°, 45°, 90°, 135°)$ with selective rearing (reared orientation: 135°).

experienced orientation (135°) is overrepresented in this case. Further it is also seen that orientations which have never been 'seen' by the cortex also have representations. Explicitly, though the system is reared with only gratings oriented at 135°, neurons responding to other orientations (of 0°, 45° and 90°) also have substantial representation depending upon the value of $\mathscr{P}$.

Moreover, the comparison of Fig. 12 with Fig. 13 also brings out the *instructive role* that visual experience plays in development. That is, visual experience *forces* a shift of orientation preference toward the experienced orientation in the DAEO phase (i.e., the post-eye-opening regime). This conclusion is based on the following observation: *although the cortical orientation preferences are rigid in the sense that unseen orientations also have representations, visual experience does alter the neuronal responses of cortical cells.*

5.5. Biological consistency

Having analyzed the results corresponding to selective rearing, we now turn to the demonstration of the consistency of these results with biological data. In the course of analyzing the influence of experience on orientation maps in the cat's visual cortex, Sengpiel et al. [15] conclude that visual experience has an instructive role on the development process, as evident from the shift of certain neuronal preferences towards

the reared orientation. Further, they also show that the cortex does have a representation of orientations which have never been reared for. Finally, they conclude ([15, pp. 731]):

> The shift of orientation preferences we observed therefore implies a competition of different orientations for cortical territory similar to the competition of thalamocortical afferents from the two eyes for terminal space in the primary visual cortex.
>
> Taken together, our results show that there is a delicate balance between a considerable intrinsic component in determining the layout of orientation preference maps and environmental factors that can modify neuronal response properties such as orientation preference.

Based on the above results and observations, we conclude that the proposed model and its results are consistent with biological data. Explicitly, the model predicts the effects of selective rearing and takes into account biological realities as follows:

(1) It shows that unreared orientations also have representation in the cortex, thus modelling its relative rigidity.
(2) It indicates an over-representation of the reared orientation, thereby bringing out the instructive role of visual experience in orientation development.
(3) It involves, explicitly, two kinds of competitions as hypothesized in [15] which are (see also Section 2.2.1): (a) Competition of a given orientation for cortical space, and (b) competition among ON- and OFF-LGN neurons for terminal space on cortical neurons.
(4) The delicate balance between intrinsic and environmental influences on the preference map is determined by the parameter $\mathscr{P}$ which controls the onset of visual experience. If $\mathscr{P}$ is low, the balance tilts towards the intrinsic component (spontaneous neural activity), and if it is high, it tilts towards visual experience. The exact value of $\mathscr{P}$ required to maintain *biological balance* is determined below.

As explained above, the parameter $\mathscr{P}$ governs the delicate balance between intrinsic and environmental influences on the developing cortex. We now turn to the following question: *For what value of* $\mathscr{P}$, *does the model prediction exactly match the biological data*? The answer to this question lies in Sengpiel et al.'s observation that, with selective rearing, *the cortical area devoted to the reared orientation is* (*approximately*) *twice the size of the orthogonal one* [15]. Now, we reformulate our question as: For what value of $\mathscr{P}$ does the experienced orientation occupy twice the cortical area of that occupied by its orthogonal orientation?.

In order to arrive at the answer, we plot $\mathscr{R}$, defined as

$$\mathscr{R} = \frac{\text{No. of neurons responding to the reared orientation}}{\text{No. of neurons responding to its orthogonal orientation}},$$

as a function of $\mathscr{P}$. The plot is shown in Fig. 14. It is observed that in the case where $\mathscr{P} = 90$, which is Miller's analysis, the ratio is equal to one. However, as $\mathscr{P}$ decreases, the reared orientation starts occupying an increasingly higher amount of cortical space (as indicated by the increase in $\mathscr{R}$). In order to match the requirement of $\mathscr{R} = 2$, we find from the graph that $\mathscr{P}$ has to be around 83.

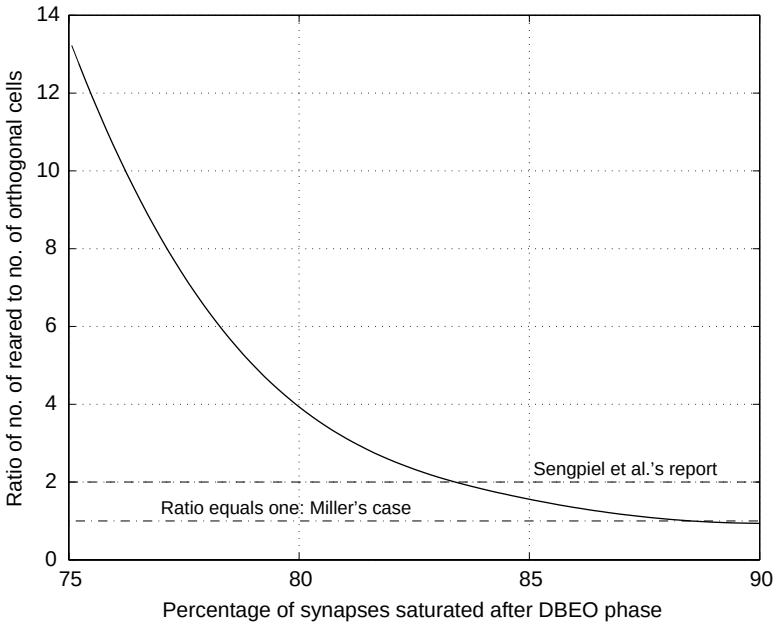

Fig. 14. Plot showing the variation of the ratio of the number of cells corresponding to the reared orientation to that of the orthogonal orientation as a function of $\mathscr{P}$.

Moreover, the observation of [15] that unseen orientations (during selective rearing) also have representation in the cortex also raises the question on the durations of the critical periods of various neurons in a cortical area. The observation may be interpreted as follows: *certain neurons in the cortical area get committed*, *and are not perturbed by environmental influences*, *while some other neurons are perturbed.* It would be interesting to examine whether the Hypothesis B can be employed to explain this phenomenon of partial influence. Explicitly, if, according to the hypothesis, the critical periods of individual neurons are local, then it is possible that certain neurons reach the end of their critical periods while certain others do not.

6. Discussions

In this section, we analyze the effects of varying model parameters, compare the model with those in the literature, and finally conclude the paper with answers to the motivating questions posed in Section 1.

6.1. Effects of parameter variations

To recall, the major parameters involved in the simulation are (i) *neighborhood parameter*, σ_n; (ii) *grating frequency range*; (iii) *range of orientations presented*;

(iv) *phase of the input sinusoids*; (iv) $\mathscr{P}$ and (v) *plasticity parameter*, η. The effects of varying σ_n were discussed in Section 3.1, and those of the frequency and orientation ranges were analyzed in Section 5. The effects of varying $\mathscr{P}$ under normal and selective rearing were brought out in Section 3.2 and Section 5, respectively.

Of the other parameters, it is observed that setting the phase of the sinusoid to some constant value (rather than making it random) does not bring out any significant change in the organization of the receptive field profile. Also, the parameter controlling the maximal synaptic value, $S_{\max}$, does not have any effect on the organization or the receptive field properties of the model cells. Varying η produces effects equivalent to increasing the amount of interaction in the neighborhood. This is because, in Eq. (14), $\eta\mathscr{K}(\mathbf{x},\mathbf{w})$ may be considered as the term which modulates plasticity. So, if η is increased, the amount of neighborhood interaction increases. However, large increases in η lead to clutter in the developed RFs.

In effect, the parameters that affect the simulation may be grouped into three sets: (i) *those which affect preference organization*: η, $\mathscr{P}$, σ_n, θ_h and θ_l; (ii) *those which affect the degree of orientation selectivity*: $\mathscr{P}$, ω_h and ω_l; and (iii) *those which do not have significant effect on both*: phase (ϕ) of the input sinusoid, and $S_{\max}$.

6.2. Comparison with other models

Comparing the proposed model with those in the literature, we find that most of the computational models in the literature deal *separately* with either (a) map development *or* (b) the development of orientation selectivity in the pre-natal phase *or* (c) an understanding of the abnormal rearing of animals. The proposed model, on the other hand, analyzes **all** these effects *together*, since the formulation (in Section 3) spans both the pre- and post-natal environments.

To be more explicit, as far as the development of orientation selectivity (RFs and preference maps together) is concerned, the results of the paper seem to be the *first attempt ever* to (i) model it, spanning the pre- and post-natal regimes; (ii) quantify the relative effects of innate and environmental factors; (iii) quantify the critical period phenomenon; and (iv) analyze the outcomes of selective and dark rearing experiments, and compare them with those on animals. Further, we have shown that the model's outcomes are consistent with biological realities with respect to normal rearing (with bounds on σ_n—Section 3.1), dark rearing (with short periods) and selective rearing (in modelling the relative rigidity of the cortex and in quantifying the balance between spontaneous neural activity and visual experience).

The limitations of the proposed model, most of which are common to Miller's basic model, are:

- It does not take into account the receptive field scatter, cortical point spread, and the multilayer architecture of the cortex.
- The vertical dimension of the cortex is not taken into account.
- The model is not realistic since modifiable intra-cortical synapses have not been taken into account.

- Determinants of the critical period duration, *like neurotrophins*, *NMDA receptors and inhibitory circuitry*, have to be modelled more appropriately.
- Feedback connections from the PVC to the LGN are not taken into account.
- The model predicts correctly the outcome corresponding to dark rearing of a shorter duration. But, it fails in the case where it is subjected to visual deprivation through the end of the critical period. To be precise, it *freezes* orientation selectivity with dark rearing whereas biology shows that orientation selectivity deteriorates if the eyes are not allowed to open [8,19].

In this context, for a comparison of the basic Miller's model (on which the model is built upon) with other models, see [6,13,16].

6.3. Conclusions

In the course of modelling the cortical, simple-cell receptive fields, we have analyzed a correlation framework with sinusoidal inputs. After examining the inability of a Miller-type rule for environments with varied input activity patterns, we propose a Kohonen-type modulation to the correlation-based plasticity equation. Since such a dynamics requires a response-dependent modulation, we employ biologically plausible response functions for the neurons in the LGN and the primary visual cortex.

The analyzed plasticity dynamics entails two kinds of competitions: (a) competition among the ON- and OFF-LGN channels to define the ON, OFF subregions in the cortical RF; and (b) competition among the cortical neurons to represent a particular orientation.

By *interpreting* the initialization of Kohonen-type dynamics with developing Miller's RFs to represent a unified pre-natal–post-natal developmental model, we quantify the relative dependence of the developmental process on spontaneous neural activity and visual experience. We have further analyzed the variations in RF properties and preference maps that arise out of a tilt in the delicate balance between spontaneous activity and visual experience. Explicitly, we have analyzed the following: (i) critical period, (ii) dark rearing, and (iii) selective rearing. We have shown that the model measures upto the biological data, and by calibrating the model performance against biological data, we have estimated bounds for certain parameters.

Finally, it is interesting to note that the inferences drawn from the simulation results based on the proposed model also provide answers to the motivating questions posed in Section 1:

(1) *Questions* 1 *and* 3: There is a sharpening in the degree of orientation selectivity of the receptive fields with the onset of visual experience. Organization can undergo substantial modification depending upon various factors, like the neighborhood definition and the onset of visual experience. Elongation in the RF subregions is also observed. Cases of simulations where only selectivity improves and organization undergoes little changes are also presented.

In order to account for the biological observation that orientation preferences *do not* undergo rearrangement under normal rearing, we have shown that the parameter σ_n has to be small.

(2) *Question* 2: It has been found that a mechanism similar to that of Miller's does not apply *directly* to the case after eye-opening. In the present work, modifications involving a competition among cortical neurons, for representing a given orientation, effectively model the development after eye-opening. The biological plausibility of such a competition has also been analyzed.

In order to account for variations in the visual environment, a response-dependent update has been proposed to give a Kohonen-type modulation to the correlation-based plasticity rule. An analysis of the possibility of such a response-dependent update is also presented.

(3) *Question* 4: We have shown that the process of saturation of synapses is a quantification of the critical period phenomenon. Higher the percentage of saturation of synapses, closer the system is to the end of its critical period.

(4) *Question* 5: The model analyzes the relevance of the hypothesis that "individual neurons have their own critical periods dependent upon the local concentration of certain chemicals". By analyzing the hypothesis with known facts about critical periods, and comparing it with models considering the local structure of neurotrophins, we show that the above hypothesis could be a plausible one.

(5) *Question* 6: It is found that the statistics of preferences do follow that of the input gratings, subject to the commitments already made as a consequence of pre-natal development. This is in agreement with the observation of [15] that the orientations never seen by the cortex also have representation in the cortical surface.

On the question of the model conforming to biological realities, we have demonstrated that:

- The model is capable of quantifying the relative rigidity of the cortex with respect to selective rearing. The model's results, compared to those of animals, indicate that orientations, which have never been 'seen' also have a representation in the cortex.
- The model is capable of quantifying the over-representation of the reared frequency in the cortex, thereby confirming the predicted 'active' role of visual experience by [15].

(6) *Question* 7: Comparing our results on selective rearing with those of [15], we have arrived at a specific value for the parameter $\mathscr{P}$ that models the delicate balance between spontaneous activity and visual experience. The parameter is also shown to control the relative rigidity of the cortex with respect to selective rearing.

Acknowledgements

The authors wish to express grateful thanks to the reviewers for their valuable comments and suggestions.

References

[1] N. Berardi, T. Pizzorusso, L. Maffei, Critical periods during sensory development, Current Opinion Neurobiol. 10 (2000) 138–145.

[2] B. Chapman, M.P. Stryker, Development of orientation selectivity in ferret visual cortex and effects of deprivation, J. Neurosci. 13 (1993) 5251–5262.
[3] B. Chapman, M.P. Stryker, T. Bonhoeffer, Development of orientation preference maps in ferret primary visual cortex, J. Neurosci. 16 (1996) 6443–6453.
[4] M.C. Crair, Neural activity during development: permissive or instructive? Current Opinion Neurobiol. 9 (1999) 88–93.
[5] M.C. Crair, D.C. Gillespie, M.P. Stryker, The role of visual experience in the development of columns in the cat visual cortex, Science 279 (1998) 566–570.
[6] E. Erwin, K. Obermayer, K. Schulten, Models of orientation and ocular dominance columns in the visual cortex: a critical comparison, Neural Comput. 7 (1995) 425–468.
[7] D. Ferster, K.D. Miller, Neural mechanisms of orientation selectivity in the visual cortex, Ann. Rev. Neurosci. 23 (2000) 441–471.
[8] Y. Fregnac, M. Imbert, Development of neuronal selectivity in the primary visual cortex of the cat, Physiol. Rev. 64 (1984) 325–434.
[9] A.E. Harris, G.B. Ermentrout, S.L. Small, A model of ocular dominance column development by competition for trophic factor: Effects of excess trophic factor with monocular deprivation and effects of antagonist of trophic factor, J. Comput. Neurosci. 8 (2000) 227–250.
[10] D.J. Heeger, Half-squaring in responses of cat simple cells, Visual Neurosci. 9 (1992) 427–443.
[11] T. Kohonen, Self-Organizing Maps, Second Edition, Springer, Berlin, 1997.
[12] Kristine Krug, C.J. Akerman, I.D. Thompson, Responses of neurons in neonatal cortex and thalamus to patterned visual stimulation through the naturally closed lids, J. Neurophysiol. 85 (2001) 1436–1443.
[13] K.D. Miller, A model for the development of simple cell receptive fields and the ordered arrangement of orientation columns through activity dependent competition between ON- and OFF-center inputs, J. Neurosci. 14 (1994) 409–441.
[14] K.D. Miller, E. Erwin, A. Kayser, Is the development of orientation selectivity instructed by activity? J. Neurobiol. 41 (1999) 44–57.
[15] F. Sengpiel, P. Stawinski, T. Bonhoeffer, Influence of experience on orientation maps in cat visual cortex, Nature Neurosci. 2 (8) (1999) 727–732.
[16] N.V. Swindale, The development of topography in the visual cortex: A review of models, Network: Comput. Neural Systems 7 (1996) 161–247.
[17] M. Weliky, L.C. Katz, Disruption of orientation tuning in visual cortex by artificially correlated neuronal activity, Nature 386 (1997) 680–685.
[18] L.E. White, D.M. Coppola, D. Fitzpatrick, The contribution of sensory experience to the maturation of orientation selectivity in ferret visual cortex, Nature 411 (2001) 1049–1052.
[19] T.N. Wiesel, D.H. Hubel, Comparisons of the effects of unilateral and bilateral eye closure on single unit responses in kittens, J. Neurophysiol. 28 (1965) 1029–1040.

N. Rishikesh obtained his Bachelor of Engineering (First class with distinction) at the Madurai Kamaraj University, Madurai, India, in 1995. He holds the Gold medal from the college and is also a university rank-holder. He completed his Master of Science (Research) in the Department of Electrical Engineering, Indian Institute of Science, Bangalore, India, in 1997. Currently, he is a doctoral student, working on biological information processing. His research interests include Neural Networks, Computer Vision and Computational Neuroscience.

Y.V. Venkatesh got his Ph.D. from the Indian Institute of science for a dissertation on the stability analysis of feedback systems. He was an Alexander von Humboldt Fellow at the Universities of Karlsruhe, Freiburg and Erlangen, Germany; National Research Council Fellow (USA) at the Goddard Space Flight Center, Greenbelt, Maryland; Visiting Fellow at the Australian National University, to name a few. His research monograph on stability and instability analysis of linear-nonlinear time-varying feedback systems has appeared in the Springer Verlag Physics Lecture Notes Series. His present work is on signal representation using wavelet-like arrays, reconstruction from partial information (like zero-crossings), and neural architectures for pattern recognition. He is a Professor at the Indian Institute of Science, Bangalore, India. He is a Fellow of the Indian National Science Academy, Indian Academy of Sciences and the Indian Academy of Engineering.